THE JOURNAL OF PHYSICAL CHEMISTRY B

Article

pubs.acs.org/JPCB

Anion Effects on Kinetics and Thermodynamics of CO_2 Absorption in Ionic Liquids

Maria Gonzalez-Miquel,[†] Jorge Bedia,[‡] Concepcion Abrusci,[§] Jose Palomar,*[,‡] and Francisco Rodriguez[†]

[†]Departamento de Ingeniería Química, Universidad Complutense de Madrid, 28040 Madrid, Spain

[‡]Departamento de Química Física Aplicada (Sección de Ingeniería Química), Universidad Autónoma de Madrid, Cantoblanco, 28049 Madrid, Spain

[§]Departamento de Biología Molecular, Universidad Autónoma de Madrid, Cantoblanco, 28049 Madrid, Spain

Supporting Information

ABSTRACT: A thermogravimetric technique based on a magnetic suspension balance operating in dynamic mode was used to study the thermodynamics (in terms of solubility and Henry's law constants) and kinetics (i.e., diffusion coefficients) of CO_2 in the ionic liquids [bmim][PF_6], [bmim][NTf_2], and [bmim][FAP] at temperatures of 298.15, 308.15, and 323.15 K and pressures up to 20 bar. The experimental technique employed was shown to be a fast, accurate, and low-solvent-consuming method to evaluate the suitability of the ionic liquids (ILs) to be used as CO_2 absorbents. Thermodynamic results confirmed that the solubility of CO_2 in the ILs followed the order [bmim][FAP] > [bmim][NTf_2] > [bmim][PF_6], increasing with decreasing temperatures and increasing pressures. Kinetic data showed that the diffusion coefficients of CO_2 in the ILs followed a different order, [bmim][NTf_2] > [bmim][FAP] > [bmim][PF_6], increasing with increasing temperatures and pressures. These results evidenced the different influence of the IL structure and operating conditions on the solubility and absorption rate of CO_2, illustrating the importance of considering both thermodynamic and kinetic aspects to select adequate ILs for CO_2 absorption. On the other hand, the empirical Wilke−Chang correlation was successfully applied to estimate the diffusion coefficients of the systems, with results indicating the suitability of this approach to foresee the kinetic performance of ILs to absorb CO_2. The research methodology proposed herein might be helpful in the selection of efficient absorption solvents based on ILs for postcombustion CO_2 capture.

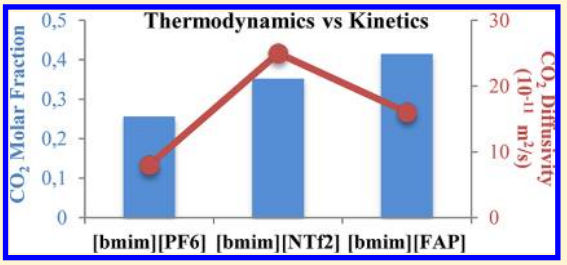

1. INTRODUCTION

CO_2 emissions from fossil-fuel-fired power plants are considered the main contributor to global climate change.[1] Conventional technologies for CO_2 postcombustion capture are based on amine solutions, which involve several concerns, such as their corrosive nature and volatility, high operational cost, and environmental impact.[2]

Over the last years, ionic liquids (ILs) have generated increasing attention in a wide variety of engineering applications, including their role as alternative solvents in gas absorption/separations processes owing to their unique physicochemical properties such as low vapor pressure and tailorability.[3−6] In particular, ILs have been proposed as potential candidates for CO_2 postcombustion capture in order to develop novel absorption technologies capable of overcoming the drawbacks associated with the amine-based systems.[7−10]

The thermogravimetric technique has been proven to be an effective method to accurately determine the absorption isotherms of CO_2 in ILs.[11−13] Indeed, this method has been intensively used by different research groups to provide systematic information about the thermodynamics of CO_2 in ILs considering the effect of the solvent structure and operating conditions.[14−22] The main results of CO_2 absorption in ILs emphasize that the anion plays a major role in the solvent structure for CO_2 absorption, with fluorination helping to increase the physical solubility of CO_2 in ILs,[15,17,23,24] and report the effect of the absorption temperature and pressure on the CO_2 solubility.[14,25−28]

The importance of the diffusion coefficients in mass transfer operations, such as the process of CO_2 absorption, is well recognized. However, although great efforts are being carried out to explain the solubility behavior of CO_2−IL systems, scarce kinetic data are available. Shifflet and Yokozeki reported the diffusion coefficients of CO_2 in [bmim][PF_6] and [bmim][BF_4] from thermogravimetric time-dependent absorption data by using a simple diffusion model.[11] Chen et al. characterized the kinetics of CO_2 in various ILs by defining an absorption rate parameter through thermogravimetric analysis.[13] A few other methods have been studied to determine the diffusion coefficients of CO_2 in ILs, such as the semi-infinitive volume approach reported by Camper et al.,[29] the employment of a lag-time technique over immobilized ILs suggested by Morgan et al.,[30] the use of a transient thin-liquid method

Received: January 23, 2013
Revised: February 18, 2013

   dx.doi.org/10.1021/jp4007679 | J. Phys. Chem. B XXXX, XXX, XXX−XXX

described by Moganty and Baltus,[31] and the use of online FTIR measurements proposed by Kortenbruck et al.,[32] whose results show that the values of the diffusion coefficients are significantly dependent on the measurement technique, although they present concordant orders of magnitude.

In our previous works, a multiscale research methodology was followed to study gas separation processes based on ILs. The absorption behavior of several gases in ILs, such as CO_2,[24,33,34] NH_3,[35,36] toluene,[37] and other VOCs,[38] was analyzed from a molecular point of view based on quantum-chemical COSMO-RS simulations to preliminarily select a set of absorbents with favorable characteristics. Moreover, thermodynamic and kinetic data were determined from thermogravimetric measurements at atmospheric pressure for the cases of NH_3[35,36] and toluene.[37] The results showed a remarkably different dependence of gas solubility and absorption rates on IL structure and operating conditions. As a consequence, it is of great interest to set up experimental procedures that accurately measure both thermodynamic and kinetic data of CO_2 in ILs, which provide the design parameters (i.e., gas−liquid equilibrium data and diffusion coefficients) required for gas separation process development. In addition, the application of a theoretical approach to foresee the absorption rate of CO_2 in IL may be helpful to consider kinetic criteria in the preliminary selection of the absorbent. In this sense, the empirical Wilke−Chang model was successfully applied to predict the diffusion coefficients of NH_3[36] and toluene[37] in ILs. Hence, by using the overall research methodology, which combines both theoretical and experimental studies, a selection of potential ILs to absorb CO_2 can be made, taking into account both thermodynamic and kinetic aspects for further development of CO_2 absorption processes.

In particular, the first aim of this contribution is to present an experimental procedure to provide accurate experimental information about the thermodynamic and kinetic behavior of CO_2 absorption in ILs as a function of the structure of the anion at different operating conditions of temperature and pressure. The second aim is to evaluate the possibility of using an empirical correlation to predict the diffusion coefficient of CO_2 in ILs. Experimental thermogravimetric measurements were performed in dynamic mode to determine the absorption isotherms and kinetic curves of CO_2 in three ionic liquids, i.e., [bmim][PF_6], [bmim][NTf_2], and [bmim][FAP], at temperatures of 298.15, 308.15, and 323.15 K and pressures up to 20 bar. These ILs have been selected because of their thermodynamically favorable CO_2 absorption capabilities.[24,33] First, the effect of the anion and the operating conditions on the thermodynamic (in terms of solubility and Henry's law constants) and kinetic (in terms of diffusion coefficients) performances of the ILs for CO_2 absorption was analyzed. In order to do so, the density of the solvents and the solubility and Henry's law constants of CO_2 in ILs were determined and compared to the available reported results to validate the experimental procedure, and the diffusion coefficients of CO_2 in each one of the solvents were determined by using a simplified diffusion mass model. Afterward, the empirical correlation of Wilke−Chang was used to estimate the diffusion coefficients of the systems, and the values were compared to those experimentally determined to evaluate the viability of using this approach to predict the kinetic behavior of a specific IL for CO_2 absorption.

2. EXPERIMENTAL PROCEDURE

2.1. Materials. Carbon dioxide, CO_2, and nitrogen, N_2, were obtained from Praxair, Inc., with a minimum purity of 99.999%. The ionic liquids l-butyl-3-methylimidazolium hexafluorophosphate, [bmim][PF_6], and l-butyl-3-methylimidazolium tris(pentafluoroethyl)trifluorophosphate, [bmim][FAP], were obtained from Merck, and the ionic liquid 1-butyl-3-methylimidazolium bis(trifluoromethanesulfonil)imide [bmim][NTf_2] was obtained from Io-Li-Tec (Ionic Liquid Technologies), all of them with a minimum purity of 99%.

2.2. Experimental Setup. The gas solubility measurements were performed with a Gravimetric High Pressure Sorption Analyzer (ISOSORP GAS LP-flow, Rubotherm). The sorption measuring instrument with magnetic suspension balance (MSB) has a measuring load of 0−10 g, and the resolution of the mass reading is 0.01 mg with a reproducibility (standard deviation) of (±) 0.03 mg and an uncertainty <0.002%. The MSB can operate in the pressure range between 10^{-6} bar (ultrahigh vacuum or UHV) and 30 bar and in the temperature range from room temperature up to 150 °C. The temperature in the sample is regulated by an external thermostat circulating bath filled with silicone oil (Julabo F25-ME), and the temperature in the measuring cell is recorded with a Pt 100 probe. The Rubotherm sorption analyzer equipment provides precise computer control and measurement of weight, pressure, and temperature to accurately determine the gas absorption−desorption isotherms and isobars. In particular, the magnetic suspension coupling control and the peripherals, which consist of the SARTORIUS Balance, JUMO DICON 400 temperature gauge, Julabo F25-ME Thermostat, DPI 282 Pressure Gauges, RUBOTHERM Gas-Dosing Unit, and BROOKS Mass Flow controller (FlowBus), are regulated by the supplied MessPro software to control the Rubotherm MSB and monitor the fully automatic process. The MSB can operate in both dynamic and static modes. Dynamic gas dosing provides a continuous flow of gas through the measuring cell and complete control of the pressure of the system. The static measurement is an optional procedure, where all dynamic mass flows and pressure control stop. All the absorption measurements in this work were performed in dynamic mode in order to ensure an exhaustive control of the set-point pressure. It should be noted that a main feature of this sorption instrument with magnetic suspension balance is the possibility of directly measuring the density of the gas phase surrounding the sample in an extremely high accuracy, which is necessary to correct the buoyancy effects acting on the sample in order to obtain reliable thermodynamic and kinetic data.

2.3. Experimental Measurements. *2.3.1. Blank Measurement.* A blank measurement was performed with the MSB in order to determine the mass and the volume of the sample container (m_{SC} and V_{SC}). The blank measurement was carried out as an adsorption isotherm without sample in the MSB (at a temperature of 298.15 K and starting from vacuum, the pressure was increased stepwise up to 20 bar with an inert gas, i.e., N_2, setting a gas flow rate of 100 mL/min). From the experimental data recorded during the blank measurement, the following linear relationship between the balance reading (m_{BAL}) and the gas density (ρ) can be written:

$$m_{BAL} = m_{SC} - \rho \cdot V_{SC} \quad (1)$$

The above linear function is the mass of the sample container in a vacuum (m_{SC}) minus the buoyancy effect ($\rho \cdot V_{SC}$). The

dx.doi.org/10.1021/jp4007679 | J. Phys. Chem. B XXXX, XXX, XXX−XXX

experimental data recorded during the blank measurement are the balance reading (m_{BAL}) and the temperature (T) and pressure (P) of the gas from which the density of the gas (ρ) can be calculated. Therefore, from the results of this blank measurement, the weight of the empty sample container (m_{SC}) and the volume of the sample container (V_{SC}) were determined.

2.3.2. Reactivation of Sample. The reactivation of the sample was performed every time after a new sample was loaded into the MSB in order to reduce its content of water and volatiles. The sample container was filled with the ionic liquid sample (≈50 mg) and loaded into the MSB. Then, the samples were dried and degassed at a temperature higher than 323.15 K while the pressure was maintained in a vacuum until the changes in mass were <0.001 mg/h.

The weight of the sample container loaded with sample (m_{SC+S}) is measured by the MSB during the reactivation procedure in a vacuum (when $P = 0$ and $\rho = 0$, then $m_{SC} = m_{BAL}$). From this data, the mass of the reactivated sample (m_S) can be calculated by subtracting from it the mass of the empty sample container ($m_S = m_{SC+S} - m_{SC}$).

2.3.3. Buoyancy Measurements. The mass of sample weighed with the MSB during the adsorption experiment needs to be corrected for the buoyancy effect acting on it in the gas phase. The buoyancy effect (B) is proportional to the product of the density and the volume of the body ($\rho \cdot V$), and becomes considerable at low temperature and high pressure.

The holding force (H), which is determined by the balance, is dependent on the equilibrium forces acting on the sample, i.e., the gravitational force (F_G) acting on the sample in earth's gravity field (g = acceleration of gravity) and the buoyancy force (B) acting on the body in the opposite direction:

$$H = F_G - B = m \cdot g - (\rho \cdot V) \cdot g \tag{2}$$

As a result of that, the balance reading ($m_{BAL} = H/g$) is equal to

$$m_{BAL} = \frac{H}{g} = m - \rho \cdot V = m_{SC+S} - \rho \cdot V_{SC+S} \tag{3}$$

The above linear function is the mass of the sample container and the sample in a vacuum (m_{SC+S}) minus the buoyancy effect, which is due to the volume of the empty sample container plus the volume of the sample (V_{SC+S}).

The buoyancy measurements were performed like absorption isotherms in the MSB (stepwise increase of pressure at constant temperature) with each one of the ionic liquids at each temperature (298.15, 308.15, and 323.15 K) under inert gas atmosphere (i.e., N_2, setting a gas flow rate of 100 mL/min). Afterward, the balance reading during the buoyancy measurement (m_{BAL}) was plotted as a function of the density of the gas (ρ) measured with the MSB. From the linear regression of the measured data, the sum of the volumes of the sample container and the sample (V_{SC+S}) is determined. Therefore, the results of the buoyancy measurement are the volume of the loaded sample container (V_{SC+S}), the volume of the sample itself ($V_S = V_{SC+S} - V_{SC}$), and the true density of the sample under the operating conditions ($\rho_S = m_S/V_S$).

2.3.4. Absorption Measurements. After the buoyancy measurement was performed, the MSB and the sample were evacuated and the isothermal absorption measurement was carried out. In particular, the CO_2 absorption isotherms in each one of the ionic liquids were determined at temperatures of 298.15, 308.15, and 323.15 K and pressures up to 20 bar. First, the system was kept under inert gas atmosphere at the set temperature until the sample mass was constant (weight change rate <0.001 mg/h). Subsequently, the CO_2 gas was introduced into the MSB (gas flow rate = 100 mL/min) and the pressure of the gas was increased stepwise at constant temperature up to the set pressure, and the increment in the sample weight was monitored and recorded. The ionic liquid and the gas were considered to have reached equilibrium when at constant pressure no further weight change was observed throughout time (weight change rate <0.001 mg/h). Afterward, the recorded balance reading (m_{BAL}) in the absorption measurement was corrected for the buoyancy effect acting on the sample and the sample container as follows:

$$m_{BAL,CORR} = m_{BAL} + \rho \cdot V_{SC+S} \tag{4}$$

This buoyancy corrected mass ($m_{BAL,CORR}$) is the mass of the sample container (m_{SC}) and the mass of the sample with absorbed gas ($m = m_S + m_{CO_2}$). Then, the mass of the sample with absorbed gas is determined by subtracting the mass of the empty sample container from this ($m = m_{BAL,CORR} - m_{SC}$), the mass of absorbed gas is calculated by subtracting the mass of reactivated sample from the mass of sample with absorbed gas ($m_{CO_2} = m - m_S$), and the molar fraction of gas absorbed is determined as follows:

$$X_{CO_2} = \frac{m_{CO_2}/M_{CO_2}}{m_s/M_{IL}} \tag{5}$$

where M_{CO_2} and M_{IL} are, respectively, the molar masses of CO_2 and the ionic liquid.

After absorption, the ionic liquids were regenerated. For the regeneration, the system was set and kept in a vacuum until the mass stabilized (weight change rate <0.001 mg/h). It was verified that the mass of the ionic liquid samples at the end of each experiment was the same as the mass initially loaded (weight change <0.2%), which was attained in less than 20 min for all the systems studied.

In this work, the temperature and the pressure were respectively controlled with uncertainties corresponding to ±0.01 K and ±0.01 bar. The maximum uncertainty of the isothermal ionic liquid density data is estimated to be below 0.002 g/cm^3, and the maximum uncertainty of the measured CO_2 mole fraction absorbed in ILs was estimated to be below 0.005.

3. RESULTS

3.1. Density. As it was exposed above, the Rubotherm sorption analyzer provides the possibility of directly measuring the density of the gas phase surrounding the sample to accurately determine the density of the solvents from the buoyancy measurements, and afterward correct the absorption data. Figure 1 shows the results obtained for the isothermal density of the ionic liquids [bmim][PF_6], [bmim][NTf_2], and [bmim][FAP] over the temperature range 298.15−323.15 K. Comparison of the ionic liquid density measurements with the available published data shows agreement within about 0.3−1.3% over the temperatures studied. Overall densities of the three ionic liquids are in the order of 1.3−1.6 g/cm^3 and present the following trend: [bmim][FAP] > [bmim][NTf_2] > [bmim][PF_6].

3.2. Thermodynamics. Experimental isothermal solubility data for CO_2 in [bmim][PF_6], [bmim][NTf_2], and [bmim]-

dx.doi.org/10.1021/jp4007679 | J. Phys. Chem. B XXXX, XXX, XXX−XXX

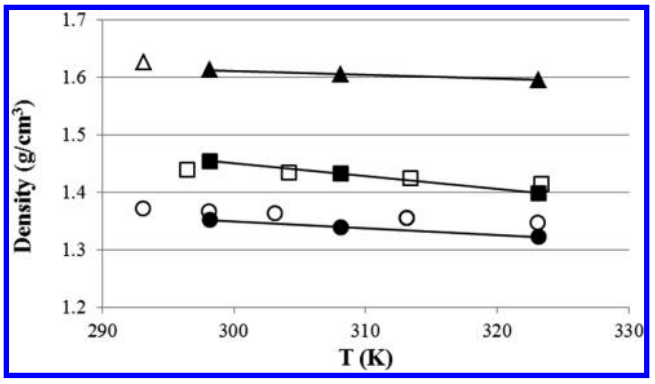

Figure 1. Density data of ionic liquids. [bmim][PF_6], measured in this work (●) and reported[39] (○); [bmim][NTf_2], measured in this work (■) and reported[50] (□); [bmim][FAP], measured in this work (▲) and reported[40] (△).

[FAP] at temperatures of 298.15, 308.15, and 323.15 K and pressures up to 20 bar are plotted in Figures 2, 3, and 4.

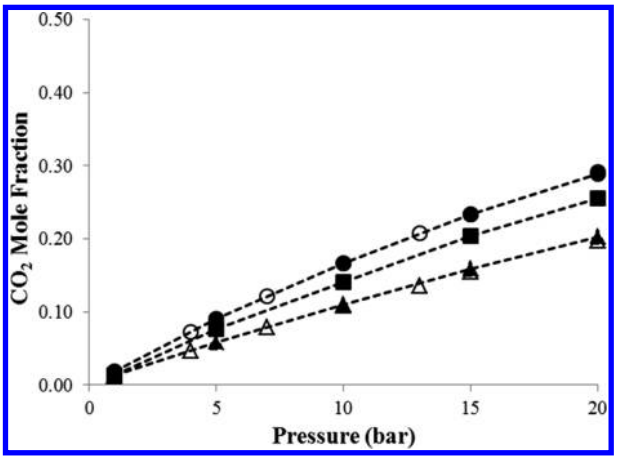

Figure 2. Isothermal solubility data of the system CO_2 and [bmim][PF_6]: measured in this work (●) and reported[11] (○) at 298.15 K; measured in this work (■) at 308.15 K; measured in this work (▲) and reported[11] (△) at 323.15 K.

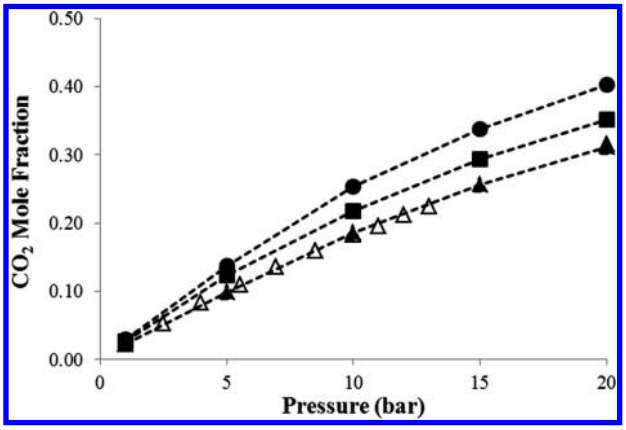

Figure 3. Isothermal solubility data of the system CO_2 and [bmim][NTf_2]: measured in this work (●) at 298.15 K; measured in this work (■) at 308.15 K; measured in this work (▲) and reported[17,41] (△) at 323.15 K.

Comparison of the measured solubilities with the previously reported values for CO_2 in [bmim][PF_6][11] and CO_2 in

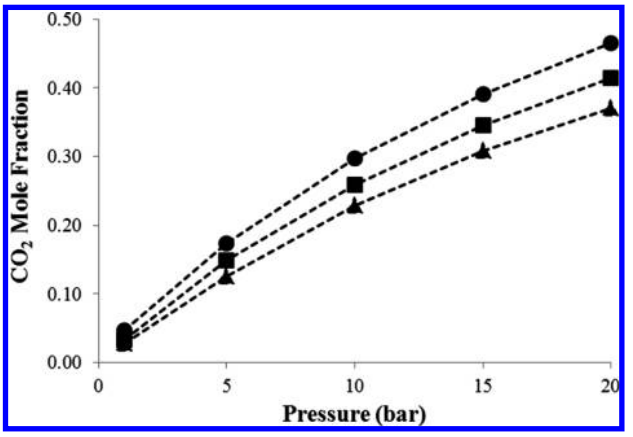

Figure 4. Isothermal solubility data of the system CO_2 and [bmim][FAP] measured in this work at (●) 298.15 K, (■) 308.15 K, and (▲) 323.15 K.

[bmim][NTf_2][17,41] determined by thermogravimetric techniques shows in Figures 2 and 3 that our data seem consistent with the available published data, and validate our experimental procedure for further solubility analyses. The obtained absorption isotherms confirm that the CO_2 solubility increases with decreasing temperature and increasing pressure for all the ILs studied. Regarding the effect of the structure of the anion, results show that the solubility of the CO_2 in the ILs containing [bmim] as a common cation follows the subsequent trend: [FAP] > [NTf_2] > [PF_6], being possible to achieve maximum molar fractions of absorbed CO_2 corresponding to 0.47, 0.40, and 0.29, respectively, at 298.15 K and 20 bar.

The Henry's law constant, K_H, is frequently used as a parameter for evaluating the solubility of a gaseous solute in a dilute solution, and it can be calculated using the following expression:

$$K_H = \lim_{x_{CO_2} \to 0} \left(\frac{P}{x_{CO_2}} \right) \quad (6)$$

where X_{CO_2} is the mole fraction of CO_2 in the IL and P is the equilibrium pressure.

According to eq 6, the measured data can be used to estimate the Henry's law constants at infinite dilution. In particular, the Henry's law constants were calculated as the slope from a linear fit of the solubility data at relatively low pressures (up to 5 bar), which provided a correlation coefficient higher than 0.99. The obtained values of the Henry's law constant of CO_2 in [bmim][FAP], [bmim][NTf_2], and [bmim][PF_6] at temperatures of 298.15, 308.15, and 323.15 K are represented in Figure 5. The results illustrate how K_H increases with the temperature and with the type of anion as follows: [FAP] < [NTf_2] < [PF_6] (note that increasing the values of the Henry's law constant involves decreasing the solubility of CO_2 in terms of molar fraction units). In addition, a comparison between the values of Henry's law constants obtained in this work and those available in the literature is shown in Figure 6, illustrating that the data determined in the present study is in agreement with the previously reported values. The measurement procedure based on the thermogravimetric technique operating in dynamic mode provides fast and accurate determination of the absorption data of CO_2 in the studied ILs, being possible to achieve the thermodynamic equilibrium of the systems in approximately 2 h for each T, P set-point.

dx.doi.org/10.1021/jp4007679 | J. Phys. Chem. B XXXX, XXX, XXX−XXX

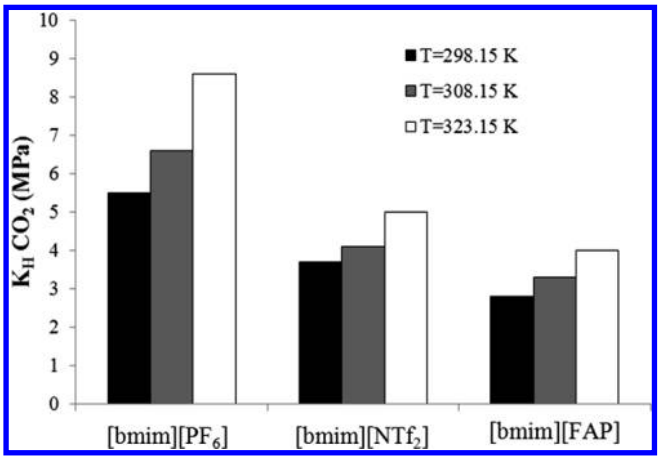

Figure 5. Henry's law constants of CO_2 in the ILs [bmim][PF_6], [bmim][NTf_2], and [bmim][FAP] at 298.15, 308.15, and 323.15 K estimated from solubility data of this work.

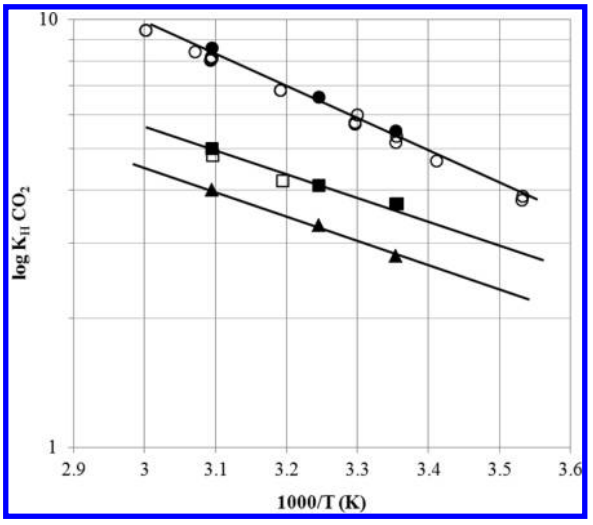

Figure 6. Comparison of estimated and reported Henry's law constants of CO_2 in ILs at different temperatures. [bmim][PF_6], estimated in this work (●) and reported[14,42−44] (○); [bmim][NTf_2], estimated in this work (■) and reported[45] (□); [bmim][FAP], estimated in this work (▲).

3.3. Kinetics. In order to evaluate the kinetics of the absorption of CO_2 in ILs, the diffusion coefficients were estimated from the time-dependent absorption data collected with the Rubotherm sorption analyzer for each one of the systems. The diffusion coefficients were estimated by applying a mass diffusion model reported by Shifflet and Yokozeki for CO_2−IL systems.[11] This model has also been used in our previous works for studying the kinetics of other gaseous solutes in ILs such as NH_3[36] and toluene.[37] Briefly, this model makes the following assumptions: the gas is dissolved in the liquid through a one-dimensional (vertical) diffusion process; the thermodynamic equilibrium is instantly established with the saturation concentration in a thin boundary layer between the gas and liquid phases; the saturation concentration, the temperature, and pressure are kept constant; and the gas−liquid system is considered a dilute solution in which the thermophysical properties of the solution do not change. Therefore, the process of gas dissolving in liquid may be described by one-dimensional mass diffusion due to the local concentration difference. The CO_2 mass balance can be written as

$$\frac{\partial C}{\partial t} = D \cdot \frac{\partial^2 C}{\partial z^2} \tag{7}$$

with an initial condition $C = C_0$ when $t = 0$ and $z < 0 < L$ and boundary conditions (i) $C = C_s$ when $t > 0$ and $z = 0$ and (ii) $\partial C/\partial z = 0$ at $z = L$. C is the concentration of gas dissolving in the IL as a function of time, t, and vertical location, z. L is the depth of IL in the container (estimated for each case using the mass of the IL sample and the corresponding density value previously determined in the buoyancy measurements), and C_0 is the initial concentration of the dissolving gas at each temperature and pressure. D is the diffusion coefficient, that is assumed to be constant. However, despite assuming a dilute solution, the CO_2 gas absorbed into the ionic liquid cannot be regarded as being highly dilute, so the diffusion coefficients must be taken as "effective" diffusion constants.

The experimentally measured quantity at a specified time is the total concentration (mass per unit volume) of dissolved gas in IL. This space-averaged concentration at a given time, $\bar{C}$, can be calculated from the equations

$$\bar{C} = \frac{1}{L}\int_0^L C \, dz \tag{8}$$

$$\bar{C} = C_s\left[1 - 2\left(1 - \frac{C_0}{C_s}\right)\sum_{n=0}^{\infty}\frac{\exp(-\lambda_n{}^2 Dt)}{L^2\lambda_n{}^2}\right] \tag{9}$$

Although the last equation contains an infinite summation, only the first few terms are sufficient in practical applications. Fitting the experimental data to this equation by nonlinear regression, the saturation concentration, C_s, and the diffusion coefficient, D, were determined for each T, P set-point. Parts A, B, and C of Figure 7, respectively, present the diffusion coefficients of CO_2 in [bmim][PF_6], [bmim][NTf_2], and [bmim][FAP] determined from the isothermal data at 298.15, 308.15, and 323.15 K and pressures from 1.0 to 20.0 bar. The order of magnitude of the diffusion coefficients is 10^{-10} to 10^{-11} m^2/s, which agrees with the available data reported by Shifflet and Yokozeki for CO_2 in [bmim][PF_6] and [bmim][BF_4] by using the thermogravimetric technique operating in static mode, under similar conditions of temperature, pressure, and mass sample.[11] The trends in the diffusivity coefficients of CO_2 in the ILs can be explained in terms of the changes in viscosities of the ILs and the CO_2−IL mixtures with the IL structure and the operating conditions. Regarding the effect of the anion, the diffusion coefficients exhibit the following order: [bmim]-[NTf_2] > [bmim][FAP] > [bmim][PF_6], a trend which agrees with the viscosity data reported for the pure ILs (Table 1). As it can be seen in the figures, in all cases, the diffusion coefficients of CO_2 in the ILs increase with absorption temperature, which can be justified from the decreasing viscosities of the solvents with increasing temperatures; however, the CO_2 solubility decreases with temperature, resulting in large but more moderate decrease in the IL viscosities,[47] which accounts for a milder increase in the diffusivity coefficients. The increase in the diffusivity coefficients with increasing operating pressures may be ascribable to the reported decreasing viscosities of the CO_2−IL mixtures with increasing CO_2 partial pressures.[47,48]

In order to compare the experimental effective diffusion coefficients with those estimated by empirical equations, the

dx.doi.org/10.1021/jp4007679 | J. Phys. Chem. B XXXX, XXX, XXX−XXX

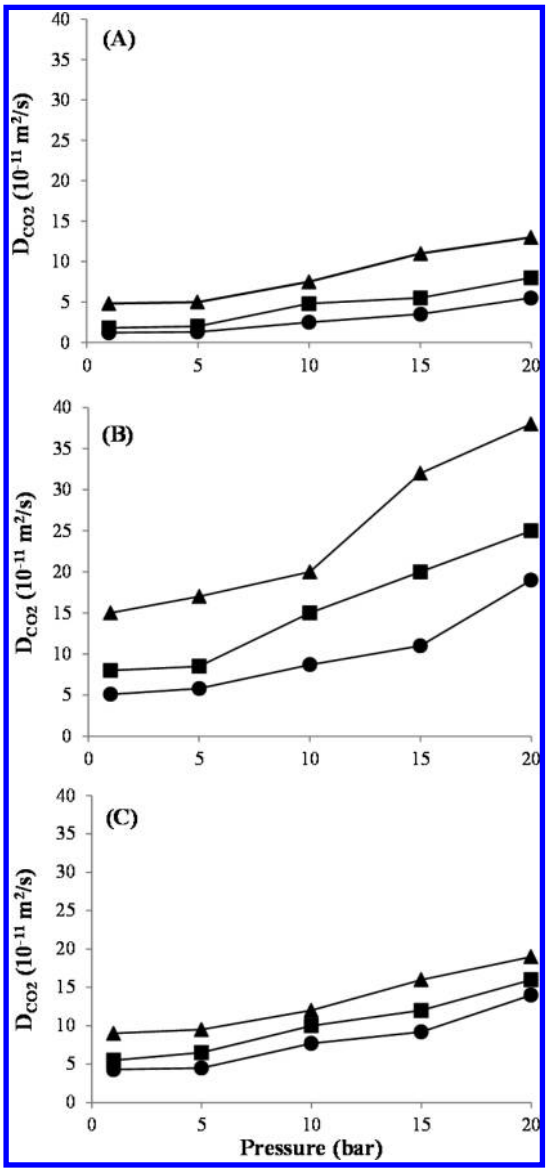

Figure 7. Diffusion coefficient of CO_2 in (A) [bmim][PF_6], (B) [bmim][NTf], and (C) [bmim][FAP] determined from thermogravimetric isothermal data from 1.0 to 20.0 bar by applying eqs 7–9: (●) 298.15 K; (■) 308.15 K; (▲) 323.15 K.

Table 1. Viscosity of the Studied ILs and the Diffusion Coefficients of CO_2 in Them Estimated by the Wilke–Chang Equation

ionic liquid	molar weight (g/mol)	T (K)	viscosity (Pa·s)	D_{CO_2} (m²/s)
[bmim][PF_6]	284.18	293.6	0.3759[a]	1.2×10^{-11}
		302.6	0.2091[a]	2.2×10^{-11}
		312.2	0.1350[a]	3.5×10^{-11}
		321.9	0.0916[a]	5.3×10^{-11}
[bmim][NTf_2]	419.37	293.4	0.0598[a]	9.0×10^{-11}
		302.9	0.0406[a]	1.4×10^{-10}
		312.4	0.0287[a]	2.0×10^{-10}
[bmim][FAP]	584.23	293.0	0.0930[b]	6.8×10^{-11}

[a]From ref 46. [b]From ref 40.

diffusion coefficients of CO_2 in ILs were also calculated using the empirical Wilke–Chang correlation[49]

$$D = 7.4 \times 10^{-8} \frac{(\phi \cdot M_{IL})^{0.5} \cdot T}{\mu \cdot V_{CO_2}^{0.6}} \quad (10)$$

where D is the diffusion coefficient (cm²/s); M_{IL} is the molecular weight of the solvent; T is the temperature (K); μ is the dynamic viscosity of the solution (cP), which will be approximated to the viscosity of the ionic liquid assuming a dilute solution; V_{CO_2} is the molal volume of solute at normal boiling point (cm³/mol); and ϕ is the association parameter with value unity for unassociated solvents.

The diffusion coefficients of CO_2 in [bmim][PF_6], [bmim][NTf_2], and [bmim][FAP] estimated by applying the Wilke–Chang equation at different temperatures are collected in Table 1. In Figure 8, the new estimated diffusion coefficients of CO_2

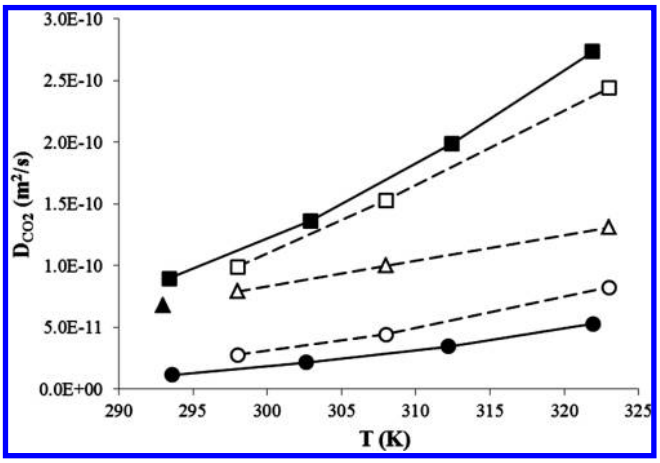

Figure 8. Comparison of diffusion coefficients of CO_2 in ILs obtained from experiments (open symbols) and estimated from Wilke–Chang correlation (filled symbols): (●) [bmim][PF6]; (■) [bmim][NTf_2]; (▲) [bmim][FAP].

in the three ILs are compared to the experimental data obtained averaged over pressures (1–20 bar). This figure shows that the diffusivity values estimated by Wilke–Chang are in reasonable agreement with the experimental data obtained for the ILs in the temperature range studied. Hence, the Wilke–Chang equation can be used as an *a priori* approach to evaluate the kinetic behavior of a potential IL candidate for CO_2 absorption.

3.4. Discussion: Thermodynamics vs Kinetics. The performance of the solvent in an absorption process depends on both thermodynamic and kinetic aspects at the operating conditions; therefore, both of them would need to be considered in the selection of suitable ILs as potential CO_2 absorbents. Figures 9–11 depict the molar fraction of CO_2 absorbed and the corresponding diffusion coefficients to illustrate the effect of the IL structure, temperature, and pressure on the CO_2 absorption process.

Figure 9 shows that the solvent which presents the best absorption capacity (i.e., [bmim][FAP]) is not the one exhibiting the highest CO_2 diffusivity (this is [bmim][NTf_2]). Figure 10 indicates that the temperature is a crucial parameter to optimize in the absorption process, since decreasing temperature increases the amount of CO_2 absorbed but decreases diffusion rates. Figure 11 shows that, for a given temperature, operating at higher pressures improves both the absorption capacity and the diffusivity. Current results indicate that the selection of the IL structure and the operating conditions should be considered in the process optimization to

dx.doi.org/10.1021/jp4007679 | J. Phys. Chem. B XXXX, XXX, XXX–XXX

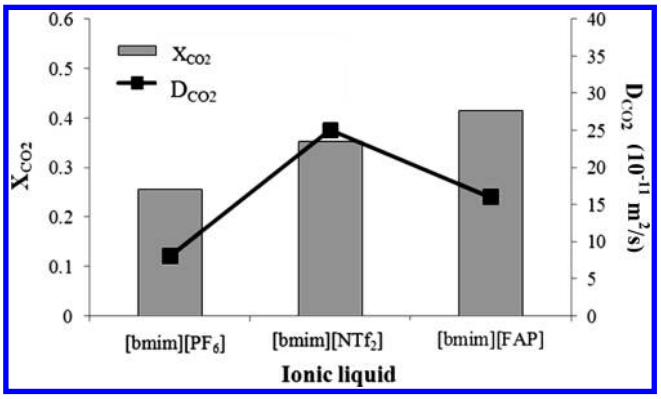

Figure 9. Effect of the anion on the solubility (mole fraction, X_{CO_2}) and diffusivity of CO_2 in ILs (T = 308.15 K and P = 20 bar).

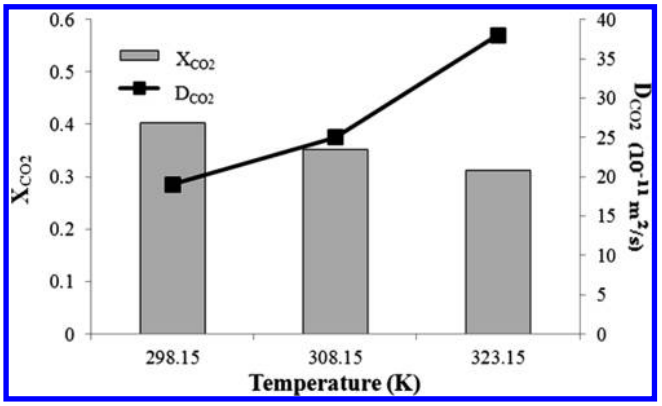

Figure 10. Effect of the temperature on the solubility (mole fraction, X_{CO_2}) and diffusivity of CO_2 in [bmim][NTf_2] at P = 20 bar.

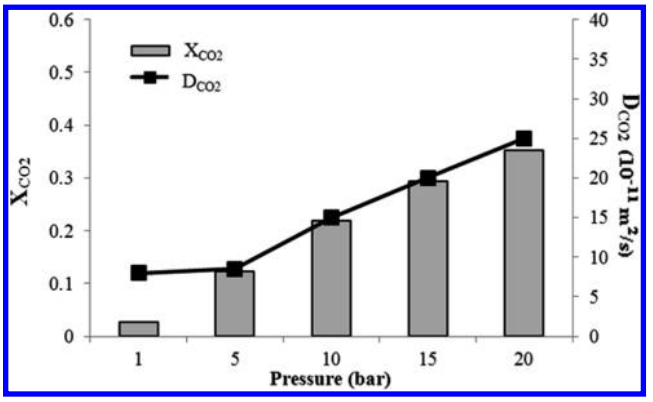

Figure 11. Effect of the pressure on the solubility (mole fraction, X_{CO_2}) and diffusivity of CO_2 in [bmim][NTf_2] at T = 308.15 K.

obtain the best balance between absorption capacity and rate in CO_2 capture operations.

4. CONCLUSIONS

A thermogravimetric technique based on a magnetic suspension balance operating in dynamic mode was used to study the thermodynamics and kinetics of CO_2 in the ionic liquids (ILs) [bmim][PF_6], [bmim][NTf_2], and [bmim][FAP] at temperatures ranging from 298.15 to 323.15 K and pressures up to 20 bar. The effect of the operating conditions and the structure of the anion on the solubility and diffusion data was reported. The proposed technique was shown to be a fast and accurate method to determine the absorption data of CO_2 in ILs, providing the possibility of directly determining the density of the samples to obtain reliable thermodynamic and kinetic data.

The isothermal densities of the ionic liquids were in the order of 1.3−1.6 g/cm^3, decreasing with increasing temperature and showing the following trend: [bmim][FAP] > [bmim]-[NTf_2] > [bmim][PF_6]. The solubility of CO_2 in the ionic liquids increased with decreasing temperatures and increasing pressures and followed the subsequent trend: [bmim][FAP] > [bmim][NTf_2] > [bmim][PF6], reaching maximum molar fractions of absorbed CO_2 corresponding to 0.47, 0.40, and 0.29, respectively, at 298.15 K and 20 bar. The diffusion coefficients of CO_2 in the ILs increased with increasing temperatures and pressures and showed the following trend: [bmim][NTf_2] > [bmim][FAP] > [bmim][FAP], presenting orders of magnitude from 10^{-10} to 10^{-11} m^2/s. Finally, the empirical Wilke−Chang correlation was successfully applied as an alternative to the diffusion model to estimate the diffusion coefficients of the systems. The results indicated the suitability of using this approach to foresee the kinetic behavior of the ILs for CO_2 absorption.

Experimental and theoretical results in this work illustrate the different thermodynamic and kinetic performance of a specific IL in the CO_2 absorption process, being a critical issue to assess both aspects in the development of industrial operations based on ILs for CO_2 capture. The methodology proposed in this work and the results obtained thereby might be helpful in the selection of appropriate solvents to develop novel absorption processes based on ILs.

■ ASSOCIATED CONTENT

Ⓢ Supporting Information

Table S1: Experimental isothermal density data of ionic liquids. Tables S2−S4: Experimental solubility data, Henry's law constants and diffusion coefficients of CO_2 in ionic liquids. This material is available free of charge via the Internet at http://pubs.acs.org.

■ AUTHOR INFORMATION

Corresponding Author

*Phone: 34 91 4976938. Fax: 34 91 4973516. E-mail: pepe.palomar@uam.es.

Notes

The authors declare no competing financial interest.

■ ACKNOWLEDGMENTS

The authors are grateful to the "Ministerio de Economía y Competitividad" and "Comunidad de Madrid" for financial support (projects CTQ2011-26758 and S2009/PPQ-1545, respectively).

■ REFERENCES

(1) IPCC. *In Climate Change 2007: The Physical Science Basis. Contribution of Working Group I to the Fourth Assessment Report of the Intergovernmental Panel on Climate Change*; Cambridge University Press: Cambridge, U.K., and New York, 2007.

(2) Rao, A. B.; Rubin, E. A. A Technical, Economic, and Environmental Assessment of Amine-Based CO_2 Capture Technology for Power Plant Greenhouse Gas Control. *Environ. Sci. Technol.* **2002**, *36*, 4467−4475.

(3) Wasserscheid, P.; Welton, T. *Ionic Liquids in Synthesis*; Wiley-VCH: Weinheim, Germany, 2003.

(4) Plechkova, N. V.; Seddon, K. R. Applications of Ionic Liquids in the Chemical Industry. *Chem. Soc. Rev.* **2008**, *37*, 123−150.
(5) Palomar, J.; Torrecilla, J. S.; Ferro, V.; Rodriguez, F. Development of an a Priori Ionic Liquid Design Tool. 1. Integration of a Novel COSMO-RS Molecular Descriptor on Neural Networks. *Ind. Eng. Chem. Res.* **2008**, *47*, 4523−4532.
(6) Palomar, J.; Torrecilla, J. S.; Ferro, V.; Rodriguez, F. Development of an a Priori Ionic Liquid Design Tool. 2. Ionic Liquid Selection through the Prediction of COSMO-RS Molecular Descriptor by Inverse Neural Network. *Ind. Eng. Chem. Res.* **2009**, *48*, 2257−2265.
(7) Huang, J.; Rüther, T. Why Are Ionic Liquids Attractive for CO_2 Absorption? An Overview. *Aust. J. Chem.* **2009**, *62*, 298−308.
(8) Bara, J. E.; Carliste, T. K.; Gabriel, C. J.; Camper, D.; Finotello, A.; Gin, D. L.; Noble, R. D. Guide to CO_2 Separations in Imidazolium-Based Room-Temperature Ionic Liquids. *Ind. Eng. Chem. Res.* **2009**, *48*, 2739−2751.
(9) Karadas, F.; Atilhan, M.; Aparicio, S. Review on the Use of Ionic Liquids (ILs) as Alternative Fluids for CO_2 Capture and Natural Gas Sweetening. *Energy Fuels* **2010**, *24*, 5817−5828.
(10) Ramdin, M.; de Loos, T. W.; Vlugt, T. H. J. State-of-the-Art of CO_2 Capture with Ionic Liquids. *Ind. Eng. Chem. Res.* **2012**, *51*, 8149−8177.
(11) Shiflett, M. B.; Yokozeki, A. Solubilities and Diffusivities of Carbon Dioxide in Ionic Liquids: [bmim][PF_6] and [bmim][BF_4]. *Ind. Eng. Chem. Res.* **2005**, *44*, 4453−4464.
(12) Soriano, A. N.; Doma, B. T.; Li, M. H. Carbon Dioxide Solubility in Some Ionic Liquids at Moderate Pressures. *J. Taiwan Inst. Chem. Eng.* **2009**, *40*, 387−393.
(13) Chen, Y.; Han, J.; Wang, T.; Mu, T. Determination of Absorption Rate and Capacity of CO_2 in Ionic Liquids at Atmospheric Pressure by Thermogravimetric Analysis. *Energy Fuels* **2011**, *25*, 5810−5815.
(14) Anthony, J. L.; Maginn, E. J.; Brennecke, J. F. Solubilities and Thermodynamic Properties of Gases in the Ionic Liquid 1-n-Butyl-3-methylimidazolium hexafluorophosphate. *J. Phys. Chem. B* **2002**, *106* (29), 7315−7320.
(15) Anthony, J. L.; Anderson, J. L.; Maginn, E. J.; Brennecke, J. F. Anion Effects on Gas Solubility in Ionic Liquids. *J. Phys. Chem. B* **2005**, *109*, 6366−6374.
(16) Anderson, J. L.; Dixon, J. K.; Brennecke, J. F. Solubility of CO_2, CH_4, C_2H_6, C_2H_4, O_2, and N_2 in 1-Hexyl-3-methylpyridinium Bis(trifluoromethylsulfonyl)imide: Comparison to Other Ionic Liquids. *Acc. Chem. Res.* **2007**, *40*, 1208−1216.
(17) Muldoon, M. J.; Aki, S. N.; Anderson, J. L.; Dixon, J. K.; Brennecke, J. F. Improving Carbon Dioxide Solubility in Ionic Liquids. *J. Phys. Chem. B* **2007**, *111*, 9001−9009.
(18) Zhang, X.; Liu, Z.; Wang, W. Screening of Ionic Liquids to Capture CO_2 by COSMO-RS and Experiments. *AIChE J.* **2008**, *54* (10), 2717−2728.
(19) Soriano, A. N.; Doma, B. T.; Li, M. H. Solubility of Carbon Dioxide in 1-Ethyl-3-methylimidazolium 2-(2-Methoxyethoxy)-ethylsulfate. *J. Chem. Thermodyn.* **2008**, *40*, 1654−1660.
(20) Soriano, A. N.; Doma, B. T.; Li, M. H. Carbon Dioxide Solubility in 1-Ethyl-3-methylimidazolium Tetrafluoroborate. *J. Chem. Eng. Data* **2008**, *53*, 2550−2555.
(21) Soriano, A. N.; Doma, B. T.; Li, M. H. Carbon Dioxide Solubility in 1-Ethyl-3-methylimidazolium Trifluoromethanesulfonate. *J. Chem. Thermodyn.* **2009**, *41*, 525−529.
(22) Yokozeki, A.; Shiflett, M. B. Separation of Carbon Dioxide and Sulfur Dioxide Gases Using Room-Temperature Ionic Liquid [hmim][Tf_2N]. *Energy Fuels* **2009**, *23*, 4701−4708.
(23) Zhang, X.; Hun, F.; Liu, Z.; Wang, W.; Shi, W.; Maginn, E. J. Absorption of CO_2 in the Ionic Liquid 1-n-Hexyl-3-methylimidazolium Tris(pentafluoroethyl)trifluorophosphate ([hmim][FEP]): A Molecular View by Computer Simulations. *J. Phys. Chem. B* **2009**, *113*, 7591−7598.
(24) Palomar, J.; Gonzalez-Miquel, M.; Polo, A.; Rodriguez, F. Understanding the Physical Absorption of CO_2 in Ionic Liquids Using the COSMO-RS Method. *Ind. Eng. Chem. Res.* **2011**, *50*, 3452−3463.
(25) Finotello, A.; Bara, J. E.; Camper, D.; Noble, R. D. Room-Temperature Ionic Liquids: Temperature Dependence of Gas Solubility Selectivity. *Ind. Eng. Chem. Res.* **2008**, *47*, 3453−3459.
(26) Kerlé, D.; Ludwig, R.; Geiger, G.; Paschek, D. Temperature Dependence of the Solubility of Carbon Dioxide in Imidazolium-Based Ionic Liquids. *J. Phys. Chem. B* **2009**, *113*, 12727−12735.
(27) Lim, B. H.; Choe, W. H.; Shim, J. J.; Ra, C. S.; Tuma, D.; Lee, H.; Lee, C. S. High-Pressure Solubility of Carbon Dioxide in Imidazolium-Based Ionic Liquids with Anions [PF_6] and [BF_4]. *Korean J. Chem. Eng.* **2009**, *26* (4), 1130−1136.
(28) Carvalho, P. J.; Alvarez, V. H.; Marrucho, I. M.; Aznar, M.; Coutinho, J. A. P. High Pressure Phase Behavior of Carbon Dioxide in 1-Butyl-3-methylimidazolium Bis(trifluoromethylsulfonyl)imide and 1-Butyl-3-methylimidazolium Dicyanamide Ionic Liquids. *J. Supercrit. Fluids* **2009**, *50*, 105−111.
(29) Camper, D.; Becker, C.; Koval, C.; Noble, R. Diffusion and Solubility Measurements in Room Temperature Ionic Liquids. *Ind. Eng. Chem. Res.* **2006**, *45* (1), 445−4450.
(30) Morgan, D.; Ferguson, L.; Scovazzo, P. Diffusivities of Gases in Room-Temperature Ionic Liquids: Data and Correlations Obtained Using a Lag-Time Technique. *Ind. Eng. Chem. Res.* **2005**, *44*, 4815−4823.
(31) Moganty, S. S.; Baltus, R. E. Diffusivity of Carbon Dioxide in Room-Temperature Ionic Liquids. *Ind. Eng. Chem. Res.* **2010**, *49*, 9370−9376.
(32) Kortenbruck, K.; Pohrer, B.; Schluecker, E.; Friedel, F.; Ivanovic-Burmazovic, I. Determination of the Diffusion Coefficient of CO_2 in the Ionic Liquid [emim][NTf_2] Using Online FTIR Measurements. *J. Chem. Thermodyn.* **2012**, *47*, 76−80.
(33) Gonzalez-Miquel, M.; Palomar, J.; Omar, S.; Rodríguez, F. CO_2/N_2 Selectivity Prediction in Supported Ionic Liquid Membranes (SILMs) by COSMO-RS. *Ind. Eng. Chem. Res.* **2011**, *50*, 5739−5748.
(34) Gonzalez-Miquel, M.; Talreja, M.; Ethier, A. L.; Flack, K.; Switzer, J. R.; Biddinger, E. J.; Pollet, P.; Palomar, J.; Rodriguez, F.; Eckert, C. A.; et al. COSMO-RS Studies: Structure−Property Relationships for CO_2 Capture by Reversible Ionic Liquids. *Ind. Eng. Chem. Res.* **2012**, *51*, 16066−16073.
(35) Palomar, J.; Gonzalez-Miquel, M.; Bedia, J.; Rodriguez, F.; Rodriguez, J. J. Task-Specific Ionic Liquids for Efficient Ammonia Absorption. *Sep. Purif. Technol.* **2011**, *82*, 43−52.
(36) Bedia, J.; Palomar, J.; Gonzalez-Miquel, M.; Rodriguez, F.; Rodriguez, J. J. Screening ILs as Suitable NH_3 Absorbents on the Basis on Thermodynamic and Kinetic analysis. *Sep. Purif. Technol.* **2012**, *95*, 188−195.
(37) Bedia, J.; Ruiz, E.; de Riva, J.; Ferro, V. R.; Palomar, J.; Rodriguez, J. J. Optimized Ionic Liquids for Toluene Absorption. *AIChE J.* **2012**, DOI: 10.1002/aic.13926.
(38) Gonzalez-Miquel, M.; Palomar, J.; Rodriguez, F. Selection of Ionic Liquids for Enhancing the Gas Solubility of Volatile Organic Compounds. *J. Phys. Chem. B* **2013**, *117*, 296−306.
(39) Harris, K. R.; Woolf, L. A.; Kanakubo, M. Temperature and Pressure Dependence of the Viscosity of the Ionic Liquid 1-Butyl-3-methylimidazolium Hexafluorophosphate. *J. Chem. Eng. Data* **2005**, *50*, 1777−1782.
(40) Merck Millipore, 2012. http://www.merckmillipore.com/showBrochure/200910.245.ProNet.pdf.
(41) Sedláková, Z.; Wagner, Z. High-pressure Phase Equilibria in Systems Containing CO_2 and Ionic Liquid of the [Cnmim][Tf_2N] type. *Chem. Biochem. Eng. Q.* **2012**, *26* (1), 55−60.
(42) Camper, D.; Scovazzo, P.; Koval, C.; Noble, R. Gas Solubilities in Room Temperature Ionic Liquids. *Ind. Eng. Chem. Res.* **2004**, *43* (12), 3049−3054.
(43) Jacquemin, J.; Husson, P.; Majer, V.; Costa Gomes, M. F. C. Low-pressure Solubilities and Thermodynamics of Solvation of Eight Gases in 1-Butyl-3-methylimidazolium Hexafluorophosphate. *Fluid Phase Equilib.* **2006**, *240* (1), 87−95.
(44) Shiflett, M. B.; Yokozeki, A. Solubility and Diffusivity of Hydrofluorocarbons in Room-Temperature Ionic Liquids. *AIChE J.* **2006**, *52* (3), 1205−1219.

(45) Zhang, J.; Zhang, Q.; Qiao, B.; Deng, Y. Solubilities of the Gaseous and Liquid Solutes and Their Thermodynamics of Solubilitation in the Novel Room-Temperature Ionic Liquids at Infinite Dilution by Gas Chromatography. *J. Chem. Eng. Data* **2007**, *52*, 2277−2283.
(46) Jacquemin, J.; Husson, P.; Padua, A. A. H.; Majer, V. Density and Viscosity of Several Pure and Water-Saturated Ionic Liquids. *Green Chem.* **2006**, *8*, 172−180.
(47) Ahosseinia, A.; Ortegab, E.; Sensenichc, B.; Scurtoa, A. M. Viscosity of n-Alkyl-3-methyl-imidazolium Bis-(trifluoromethylsulfonyl)amide Ionic Liquids Saturated with Compressed CO_2. *Fluid Phase Equilib.* **2009**, *286*, 72−78.
(48) Tomida, D.; Kenmochi, S.; Qiao, K.; Bao, Q̃; Yokoyama, C. Viscosity of Ionic Liquid Mixtures of 1-Alkyl-3-methylimidazolium Hexafluorophosphate + CO_2. *Fluid Phase Equilib.* **2011**, *307*, 185−189.
(49) Wilke, C. R.; Chang, P. Correlation of Diffusion Coefficients in Dilute Solutions. *A1ChE J.* **1955**, 264−270.
(50) Fredlake, C. P.; Crosthwaite, J. M.; Hert, D. H.; Aki, S. N. V. K.; Brennecke, J. F. Thermophysical Properties of Imidazolium-Based Ionic Liquids. *J. Chem. Eng. Data* **2004**, *49*, 954−964.